AAC Journals.ASM.org

Chemotherapy-Associated Changes of Histopathological Features of *Mycobacterium ulcerans* Lesions in a Buruli Ulcer Mouse Model

Marie-Thérèse Ruf,[a,b] Daniela Schütte,[a,b] Aurélie Chauffour,[c] Vincent Jarlier,[c] Baohong Ji,[c†] and Gerd Pluschke[a,b]

Swiss Tropical and Public Health Institute, Basel, Switzerland[a]; University of Basel, Basel, Switzerland[b]; and UPMC Université Paris 06, ER5, EA 1541, Laboratoire de Bactériologie-Hygiène, Paris, France[c]

Combination chemotherapy with rifampin and streptomycin (RIF-STR) for 8 weeks is currently recommended by the WHO as the first-line treatment for *Mycobacterium ulcerans* infection (Buruli ulcer). To gain better insight into the mode of action of these antibiotics against established *M. ulcerans* infection foci and to characterize recovery of local immune responses during chemotherapy, we conducted a detailed histopathological study of *M. ulcerans*-infected and RIF-STR-treated mice. Mice were inoculated with *M. ulcerans* in the footpad and 11 weeks later treated with RIF-STR. Development of lesions during the first 11 weeks after infection and subsequent differences in disease progression between RIF-STR-treated and untreated mice were studied. Changes in histopathological features, footpad swelling, and number of CFU were analyzed. After inoculation with *M. ulcerans*, massive infiltrates dominated by polymorphonuclear leukocytes developed at the inoculation site but did not prevent bacterial multiplication. Huge clusters of extracellular bacteria located in large necrotic areas and surrounded by dead leukocytes developed in the untreated mice. Chemotherapy with RIF-STR led to a rapid drop in CFU associated with loss of solid Ziehl-Neelsen staining of acid-fast bacilli. Development of B-lymphocyte clusters and of macrophage accumulations surrounding the mycobacteria demonstrated the resolution of local immune suppression. Results demonstrate that the experimental *M. ulcerans* mouse infection model will be a valuable tool to investigate efficacy of new treatment regimens and of candidate vaccines.

Buruli ulcer (BU) caused by *Mycobacterium ulcerans* is the third most common human mycobacterial disease of immunocompetent hosts after tuberculosis and leprosy (19, 38, 42, 43). It is a neglected emerging disease present in tropical and subtropical regions, with the highest prevalence in West African countries (2, 6). Occurrence of BU is associated with swampy areas, stagnant water bodies, or slow-flowing rivers. However, the mode of transmission and the natural reservoir of *M. ulcerans* are still not known. Contamination of wounds from environmental reservoirs, such as biofilms on aquatic vegetation or soil, and transmission via insect bites have been implicated (10, 24–27, 29, 30). An animal reservoir, possums, has been identified in a region of southern Australia (11) where BU is endemic, but so far not in Africa (9, 41).

Clinical presentation of BU starts with a painless subcutaneous nodule, papule, plaque, or edema which can later develop into ulcers with extensive necrosis and undermined edges (44). The disease primarily affects the limbs, but other body parts can also be involved. Spontaneous healing may occur, often leaving extensive scarring and deformities behind (6, 38, 43). While surgery has traditionally been the only recommended treatment for BU, the current WHO treatment recommendation is a combination chemotherapy with rifampin and streptomycin (RIF-STR) for 8 weeks for all forms of the active disease (3, 20, 28, 33, 45). Drawbacks of this combination are potential long-term side effects and the daily intramuscular (i.m.) injections required for streptomycin (37). Therefore, alternative treatment regimens are being evaluated (4).

Clumps of extracellular acid-fast bacilli (AFB) surrounded by large areas of necrosis of the deep dermal and adipose tissue associated with only minimal inflammation are characteristic histopathological features of BU (12–14, 35). Immune responses to mycobacterial infections are normally characterized by an early, acute, predominantly neutrophilic response, whereas in the chronic stage, mononuclear and granulomatous patterns develop (35). While *M. ulcerans* cells may be taken up in the early stages of infection by phagocytes, they seem to persist only transiently inside these host cells (5, 34, 36). Killing of the phagocytes by the macrolide cytotoxin mycolactone of *M. ulcerans* leads to the release of the bacteria. Subsequent extracellular multiplication results in the development of extracellular clusters of AFB inside large necrotic areas (35).

Here we have studied bacterial killing and recovery of local immune responses in a mouse model for *M. ulcerans* disease and compared these findings to features observed in human BU lesions.

MATERIALS AND METHODS

Ethics statement. In conducting the experiments, the Laboratoire de Bactériologie-Hygiène followed the official instructions for the appropriate use of animals (issued by the Direction Départementale des Services Vétérinaires de Paris and the Préfecture de Police de Paris).

Infection of mice with *M. ulcerans*. *M. ulcerans* strain CU001 isolated from a BU patient from Côte d'Ivoire was maintained through regular passage in mouse footpads. This isolate has been used in other studies evaluating the *in vivo* activities of various antimicrobial agents against *M. ulcerans* (15–18, 23). The MICs of RIF and STR for strain CU001 on 7H11 agar medium are 2 and 0.25 μg/ml, respectively (18). A total of 98 female BALB/c mice, 4 weeks old, were purchased from the Janvier Breeding

Received 16 August 2011 Returned for modification 7 September 2011
Accepted 11 November 2011
Published ahead of print 5 December 2011
Address correspondence to Gerd Pluschke, gerd.pluschke@unibas.ch.
† Deceased.

doi:10.1128/AAC.05543-11

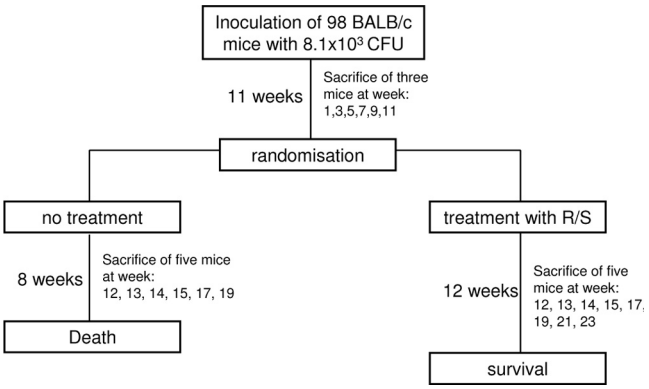

FIG 1 Study design. R/S, rifampin-streptomycin.

Center, Le Genest-Saint-Isle, France. Both hind footpads of mice were inoculated subcutaneously with 0.03 ml of a freshly prepared *M. ulcerans* suspension each. The inoculum size was 8.1×10^3 CFU per footpad.

Antibiotic treatment of mice. Rifampin (RIF) (Aventis, Paris, France) was suspended in 0.05% agar-distilled water and given by oral gavage (10 mg/kg body weight). Streptomycin (STR) (Panpharma, Fougeres, France) was diluted with normal saline and administered by subcutaneous injection (150 mg/kg body weight). Both antimicrobial agents were given once daily during weekdays (i.e., 5 times weekly) (15–18, 23).

Study design. Until week 11 after inoculation, every second week three mice were sacrificed (Fig. 1). The right footpad was used for histopathological analysis, whereas the left hind footpad was used to determine the CFU per footpad. After 11 weeks, mice were randomized and allocated among two groups: untreated control and the RIF-STR-treated group. Treatment with RIF-STR was started immediately after randomization and lasted for 12 weeks. The first 4 weeks after randomization, 5 mice each of the treated and untreated groups were sacrificed each week for histopathological analysis and determination of CFU. Afterwards, samples were taken every second week. For the untreated group, two more time points were evaluated (weeks 6 and 8 after commencement of treatment), and for the treatment group, four more time points were evaluated (weeks 6, 8, 10, and 12 after commencement of treatment) (Fig. 1).

Scoring of lesion index. Footpads were examined for determination of the lesion index directly before mice were sacrificed. The lesion index was scored from 0 to 4 as follows: 0, the footpad appeared normal; 1, the footpad showed slight swelling; 2, swelling was limited to the inoculated footpad; 3, swelling extended to the whole hind foot; and 4, swelling extended to the whole limb (Fig. 2).

Enumeration of CFU in footpads. To enumerate CFU, the tissues of the inoculated footpads were removed aseptically and homogenized in Hanks' solution in a final volume of 2 ml. For the untreated control mice, the tissue suspensions were serially diluted in 10-fold steps, and 0.1 ml of each of three appropriate dilutions was plated in triplicate on Löwenstein-Jensen medium. For the RIF-STR-treated mice, the entire volume (2 ml) of the undiluted tissue suspension from each inoculated footpad was plated on 10 tubes of Löwenstein-Jensen medium. CFU were enumerated after incubation at 30°C for 90 days.

Histopathological analyses. After mice were sacrificed, footpads were removed above the ankle and immediately fixed in neutral buffered 4% paraformaldehyde for 24 h. Afterwards, they were incubated in decalcification solution, consisting of 0.6 M EDTA and 0.25 M citric acid, for 10 days at 37°C under shaking conditions. After decalcification of bones, footpads were embedded in paraffin, cut into 5-μm sections using an HM 335 E rotary microtome (Microm International GmbH), and retrieved on Superfrost Plus (Thermo Scientific) slides. Staining with hematoxylin and eosin (HE) and Ziehl-Neelsen (ZN) was performed according to standard WHO protocols (44).

For immunohistochemistry, sections were deparaffinized and rehydrated, endogenous peroxidase was blocked with 3% H_2O_2 for 10 min, and unspecific binding was prevented by incubation with blocking serum matching the secondary antibody host. Subsequently, slides were pretreated by the hot-borate antigen retrieval method (0.02 M, pH 7) (21) and incubated at room temperature with (i) monoclonal antibodies against CD45R (B cells; clone RA3-6B2) (Serotec), monocytes/macrophages (Mo-Ma; clone MOMA-2) (Serotec), CD3 cells (T cells; clone CD3-12) (Serotec), neutrophils (clone NIMP-R14) (Abcam), and KI67 (proliferation marker; clone SP6) (Thermo Scientific) or (ii) polyclonal rabbit serum against mycobacterial (*M. leprae*) antigens (pAbLep; Colo-

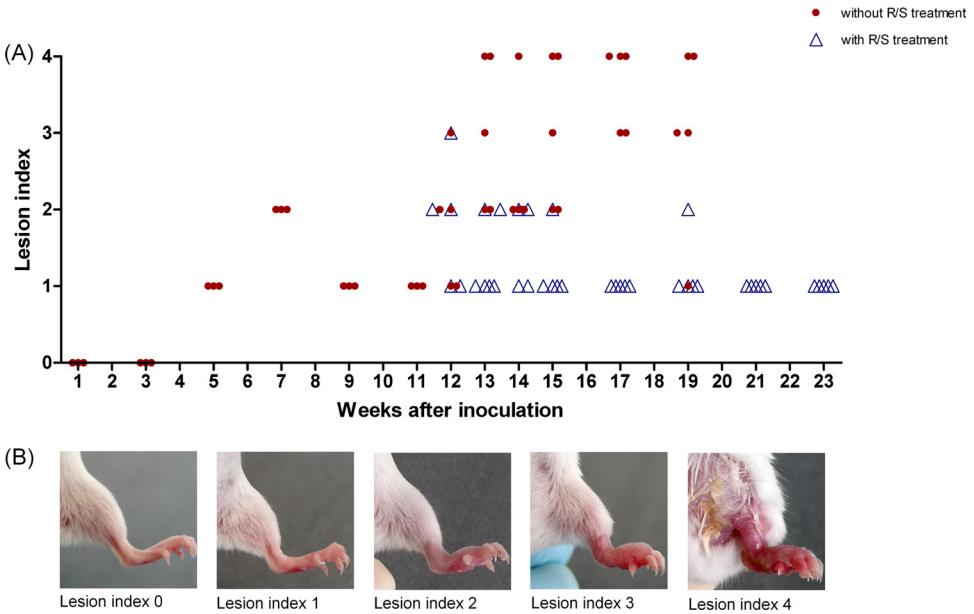

FIG 2 Evolution of the lesion index over time after infection. (A) Evolution among untreated (circles) and RIF-STR-treated (triangles) mice. (B) Representative presentations of footpads associated with different scores of the lesion index.

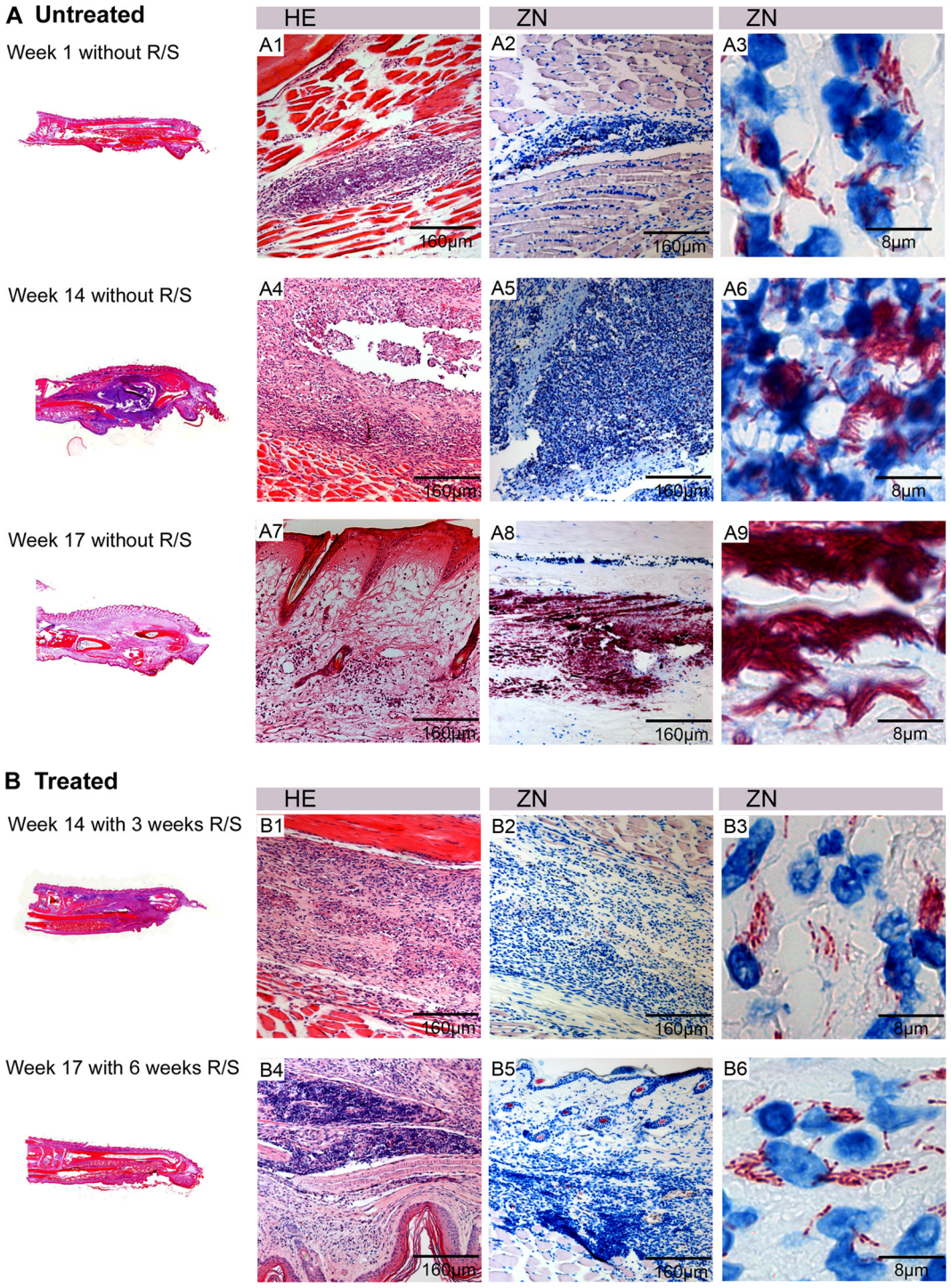

FIG 3 Overview of histopathological features of treated and untreated lesions. Shown are histological sections stained with HE (A1, A4, A7, B1, and B4) and ZN (A2, A3, A5, A6, A8, A9, B2, B3, B5, and B6) and counterstained with methylene blue. Footpads from mice without chemotherapy (A) and with RIF-STR treatment (B). (A1 to A3) Footpad 1 week after inoculation, showing slight infiltration and small numbers of intra- and extracellular bacteria. (A4 to A6) footpad 14 weeks after inoculation, showing a large infiltrated area mainly composed of destroyed PMNs surrounding large numbers of extracellular AFB. (A7 to A9) Footpad 17 weeks after inoculation without treatment, showing a large edematous necrotic area, with extracellular bacterial clusters. (B1 to B3) Footpad 3 weeks after start of treatment with RIF-STR, showing mild infiltration and AFB with beaded appearance. (B4 to B6) Footpad 6 weeks after start of treatment, showing dense lymphocyte clusters and AFB with beaded appearance.

rado State University, CO). Afterwards, sections were incubated for 30 min with a corresponding biotinylated secondary antibody (Vector Laboratories) and for an additional 30 min with streptavidin-horseradish peroxidase conjugate (Vectastain ABC kit; Vector Laboratories). Staining was performed using Vector NovaRed (Vector Laboratories) and Meyer's hematoxylin as a counterstain (Sigma). Sections were mounted with Eukitt mounting medium (Fluka). Pictures were taken with a Leica DM5000B microscope.

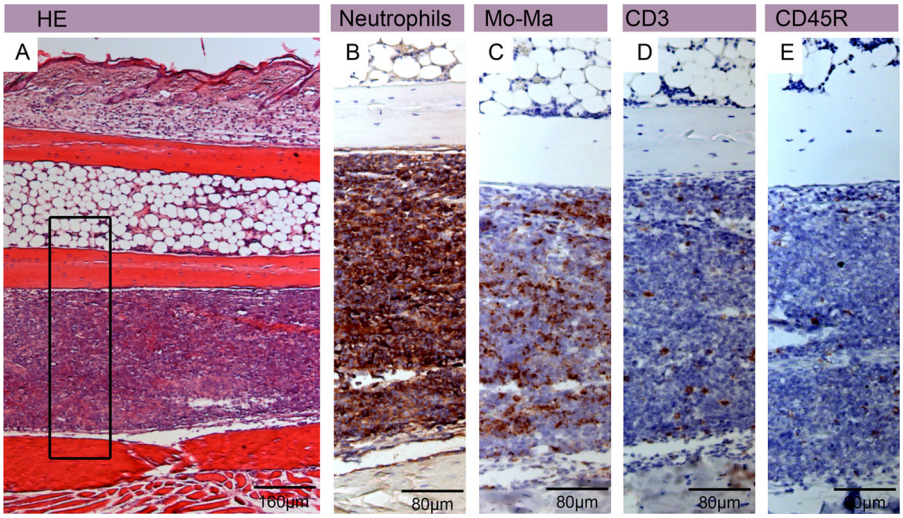

FIG 4 Neutrophilic infiltration in untreated mouse footpads early after inoculation. Shown are histological sections of a footpad from an untreated mouse 3 weeks after inoculation stained with either hematoxylin-eosin (HE) (A) or antibodies against cell surface or cytoplasmic markers and counterstained with hematoxylin (B to E). Haematoxylin-eosin staining revealed a large band of infiltrating leukocytes, mainly composed of neutrophils (B) and monocytes/macrophages (C). Only a few $CD3^+$ T cells (D) and a few $CD45R^+$ B cells (E) were found.

Based on the analysis of numerous tissue samples from lesions of Buruli ulcer patients, taken before, during, or after treatment, we selected the characteristic micrographs shown in Fig. 8.

RESULTS

Multiplication of *M. ulcerans* and tissue destruction in inoculated footpads. Eleven weeks after footpad inoculation with *M. ulcerans*, lesion indices of infected mouse footpads had increased from 0 to 1 (Fig. 2), and mice were randomized into a control group receiving no antibiotic therapy and a treatment group receiving antibiotics 5 times weekly (Fig. 1). Thereafter, the lesion indices of the group without antibiotic treatment proceeded quickly to 3 or 4 (Fig. 2). At week 19, all remaining untreated mice had to be sacrificed because the first signs of severe pathology developed. These macroscopic observations correlated well with the histopathological features. Results of the histopathological analyses are shown for representative samples and for selected time points in Fig. 3.

One week after inoculation, when the lesion index was still 0, only minor histopathological changes could be observed (Fig. 3A1 to A3). Between the muscle fibers, small clusters of infiltrating cells, mainly polymorphnuclear leukocytes (PMNs), colocalizing with the AFB were observed. AFB were found both intra- and extracellularly during this early stage of infection. Animals receiving no treatment showed a swelling of the whole footpad 14 weeks after inoculation associated with large numbers of AFB localized in accumulations of killed leukocytes (Fig. 3A4 to A6). Infiltration in untreated footpads consisted mainly of neutrophils (Fig. 4B), and monocytes/macrophages (Fig. 4C), T cells (Fig. 4D), and B cells (Fig. 4E) were rarely found at this time point of the infection: the majority of bacteria were found extracellularly between the dead leukocytes. Globus-like intracellular AFB clusters (Fig. 5A1 and A2) may represent precursors of extracellular microcolonies (5). Without antibiotic treatment, 17 weeks after infection, macroscopic swelling of footpads had extended to the ankle and the lower part of the leg (Fig. 3A7 to A9). Histopathology revealed large necrotic areas where connective tissue, muscles, and glands were completely destroyed. Neutrophilic infiltrates present earlier during the infection had largely disappeared (Fig. 3A7). Huge clusters of extracellular bacteria were primarily located in the middle of this necrotic area (Fig. 3A8 and A9). At the periphery of the extended necrotic areas containing this enormous bacterial burden, new foci were developing from spreading mycobacteria (Fig. 5A1). Here, interactions between bacterial cells and phagocytes attracted to the site of infection could be observed (Fig. 5A2). In contrast to the AFB forming the large extracellular conglomerations in the main necrotic infection focus (Fig. 5B1 and B2), more than 50% of the mycobacteria forming the new foci no longer exhibited a uniform solid ZN staining but had a "beaded" appearance (Fig. 5A3 and A4).

The epidermis above the infection foci remained intact for extended periods of time after infection, covering the necrotic dermal layer. Ulceration therefore occurred much later than footpad swelling (data not shown). Proliferation of keratinocytes in the epidermal layer was demonstrated by specific staining for the proliferation marker Ki67 (Fig. 5C1 and C2). Compared to tissue from uninfected mice this staining tended to be stronger, but due to heterogeneity within the dermis, a quantitative assessment of differences was not possible.

Response to chemotherapy. Footpad lesion indices of mice receiving antibiotic treatment from week 11 onwards increased transiently to 2 in 35% of the mice or to 3 in 5% of the mice, but from week 21 onwards, all footpads returned to an index of 1 (Fig. 2). While the right hind footpads were used for histopathological analysis, the left hind footpads were used for enumeration of CFU. Chemotherapy caused a rapid decline in the number of CFU (Fig. 6). Already after 3 weeks of treatment, four of five footpads were culture negative. However, single culture-positive footpads were still found after 6 and 8 weeks of treatment, and only after 10 and 12 weeks were all (5/5) footpads culture negative (Fig. 6). CFU counts in untreated footpads increased further (Fig. 6) until 17 weeks after inoculation when mice had to be sacrificed.

Already 3 weeks after start of chemotherapy, over 50% of the

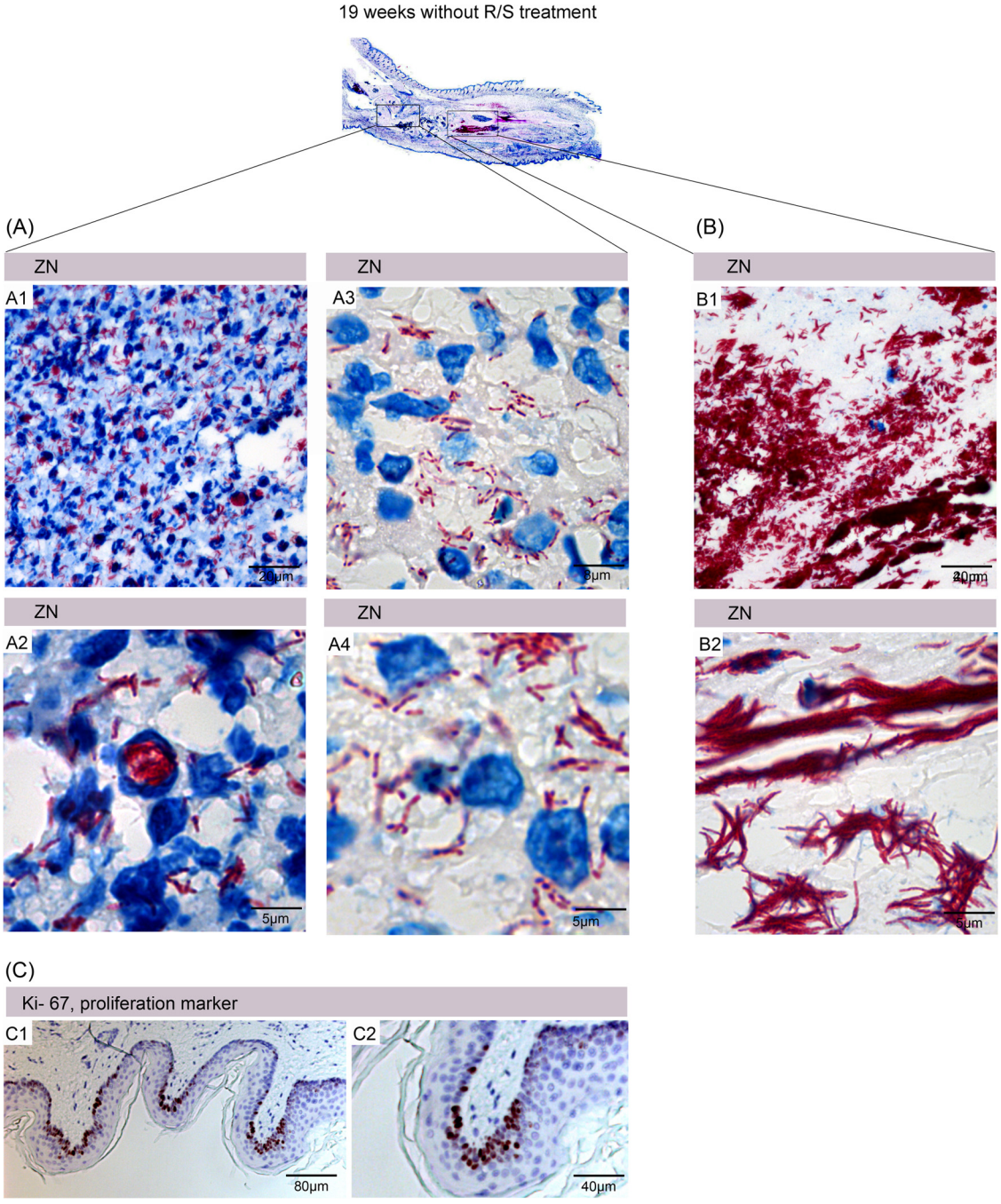

FIG 5 Appearance of mycobacteria at different times after inoculation. Shown are histological sections of the footpad from an untreated mouse 19 weeks after inoculation stained with ZN and counterstained with methylene blue (A and B) or stained with an antibody and counterstained with hematoxylin (C). The main infection focus and a more peripheral accumulation of AFB are boxed. (A1) Low-magnification picture of a peripheral AFB accumulation, showing interactions between the mycobacteria and phagocytes. (A2) Globus-like structures representing numerous intracellular AFB residing in macrophages. (A3 and A4) ZN staining of peripheral AFB reveals the presence of beaded bacteria. The main infection focus contains no viable phagocytes, but there are large extracellular clusters of AFB (B1) exhibiting solid ZN staining (B2). Staining with the proliferation marker Ki67 revealed a strong proliferative activity of epidermal keratinocytes (C1 and C2).

AFB were either internalized or associated with macrophages and neutrophils and no longer showed a uniform solid ZN staining but appeared as beaded rods (Fig. 3B2 and B3). After 8 weeks of chemotherapy, none of the intracellular (Fig. 7A1) or extracellular (Fig. 7A2) AFB showed solid ZN staining.

Three weeks after initiation of chemotherapy, footpads no longer showed major swelling or edema, although chronic infiltrates had developed (Fig. 3B1). Immunohistochemical staining revealed the formation of leukocyte accumulations mainly composed of an outer macrophage belt (Fig. 7B1 and B2) and an inner

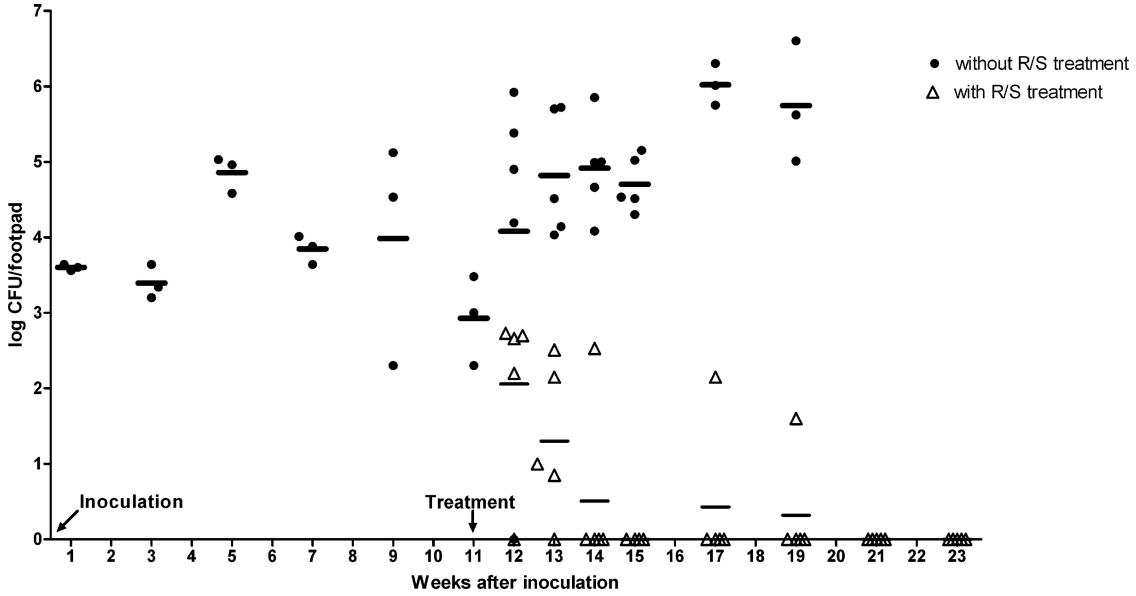

FIG 6 Changes in CFU counts after inoculation and during RIF-STR treatment. Mouse footpads were inoculated with 8.1×10^3 *M. ulcerans* CFU at week 0. The control group (●) received no treatment. In the treatment group (Δ), chemotherapy with RIF-STR (R/S) started at week 11.

belt consisting of neutrophils (Fig. 7B3) surrounding residual AFB (Fig. 7B4). Limited numbers of T cells and individual B cells were interspersed in these clusters (data not shown). While 3 weeks later the overall extent of the leukocyte infiltration had decreased, very densely packed lymphocyte clusters (Fig. 3B4) appeared in addition to the persisting beaded AFB immersed in accumulations of macrophages/neutrophils. These lymphocyte clusters (Fig. 7C1) consisted mainly of $CD45R^+$ B cells (Fig. 7C2), no macrophages (Fig. 7C4) or PMNs (Fig. 7C5), and only scattered T cells. More T cells were found in the areas surrounding the tightly packed clusters (Fig. 7C3).

DISCUSSION

Since 2004, WHO has recommended a dual antibiotic therapy with oral rifampin (10 mg/kg) and intramuscular (i.m.) streptomycin (15 mg/kg) administered daily for at least 8 weeks (45). While early BU lesions can usually be effectively managed by this antimicrobial treatment alone, more advanced lesions may require surgical débridement and/or skin grafting (3, 20, 28, 33). To contribute to a better understanding of the local responses in BU lesions, here, we performed a longitudinal histopathological study in mice experimentally infected with *M. ulcerans*. Changes in macroscopic appearance, mycobacterial load, tissue destruction, and local immune responses before and during chemotherapy were assessed.

During the establishment of infection, intracellular bacilli were observed and intracellular accumulation of AFB led to the development of globus-like structures. After killing of host cells by the macrolide toxin mycolactone, these may be efficient seeds for the large extracellular clusters of AFB that developed at later stages of the infection. Evidence for a transient intracellular stage of *M. ulcerans* and the ability to subsequently destroy the infected phagocytes has also been obtained in *in vitro* studies (5, 40). However, early immune responses may also have protective potential, since only a small proportion of individuals exposed to *M. ulcerans* seem to develop clinical disease (8). Immune status, as well as the size of the initial inoculums and the site of the initial infection may influence the outcome.

Animal studies have yielded conflicting results regarding the nature of leukocytic infiltrates in early stages of the infection. While it has been reported that neither wild-type nor mycolactone-negative *M. ulcerans* strains were strong neutrophilic attractants (1), in agreement with results reported by Coutanceau et al. (5), we observed substantial neutrophilic infiltrates during the first weeks after infection. At later stages, no viable neutrophils were left in the necrotic center of the established BU lesions, but remains of the killed neutrophils could still be detected by immunohistochemical staining. In humans, the very early stages of *M. ulcerans* infection are not associated with significant clinical signs and symptoms and have therefore never been examined histopathologically. However, massive neutrophilic infiltrates observed during the first weeks after experimental infection of mice seem to have correlates in early human disease, since remains of neutrophils are commonly found in the necrotic areas of human BU lesions (Fig. 8A to D) (32, 35).

In the mice, the epidermis above the infection foci stayed intact for extended periods of time after inoculation, covering the progressively necrotizing dermal layer. In human BU disease, epidermal hyperplasia is a characteristic feature, and elevated proliferation of keratinocytes is typically observed (Fig. 8E and F). Also, in the mice, the epidermis above the infection foci showed strong staining with the proliferation marker Ki67 (Fig. 5C). Other hallmarks of human BU lesions, such as extensive coagulative necrosis and edema formation (35) developed slowly in the mouse footpads and became only apparent in untreated mouse footpads about 14 weeks after inoculation. Since the mode of transmission of *M. ulcerans* is not clear, the incubation time in humans cannot be reliably estimated.

While the necrotic core of advanced BU lesions is typically free of viable leukocytes, accumulations of immune cells are found

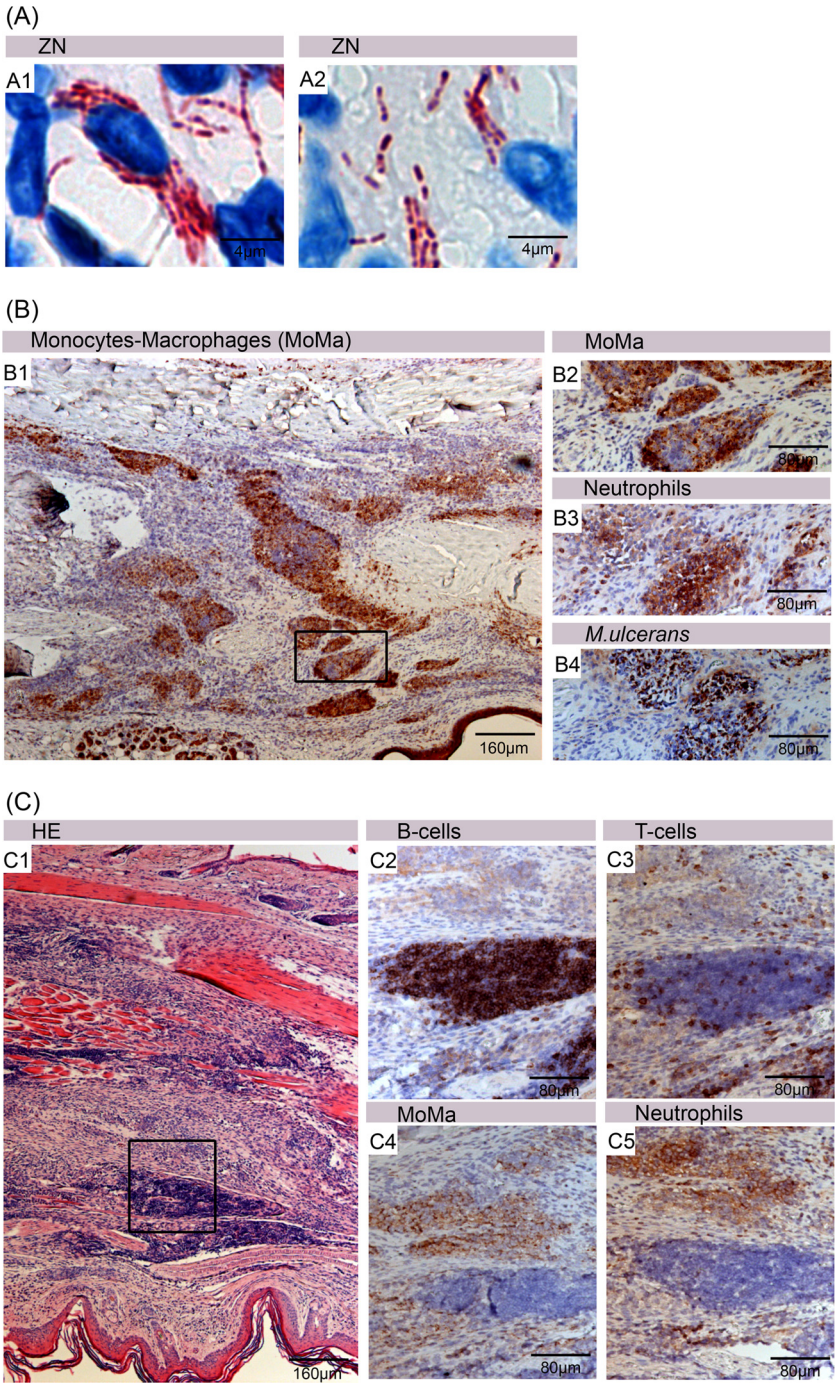

FIG 7 Inflammatory responses and development of B-cell clusters in RIF-STR-treated mice. Histological sections were either stained with ZN and counterstained with methylene blue (A1 and A2) or stained with antibodies against cell surface or cytoplasmic markers and counterstained with hematoxylin (B1 to B4 and C2 to C5), or sections were stained with hematoxylin and eosin (C1). After 8 weeks of antibiotic therapy, all intracellular (A1) as well as extracellular (A2) AFB appeared as beaded rods. Immunostaining of mouse footpads 3 weeks after commencement of antibiotic therapy revealed a strong clustering of monocytes and macrophages (Mo-Ma) (B1 and B2), neutrophils (B3), and *M. ulcerans* bacteria (B4), as well as the formation of large lymphocyte accumulations 6 weeks after commencement of antibiotic therapy (C), which were mainly composed of $CD45^+$ B cells (C2), only a few $CD3^+$ T cells (C3), and basically no macrophages (C4) or neutrophils (C5).

both in the mouse model and in human lesions (Fig. 5A and B and Fig. 8G) at the rim between the necrotic tissue and healthy tissue. Also in untreated lesions, these seem to be sites where adaptive immune responses are initiated. These may be of importance for spontaneous healing occasionally observed in both early and advanced BU disease (7, 43).

After the start of antibiotic treatment, local infiltrates switched from a predominantly unorganized neutrophilic type to a more

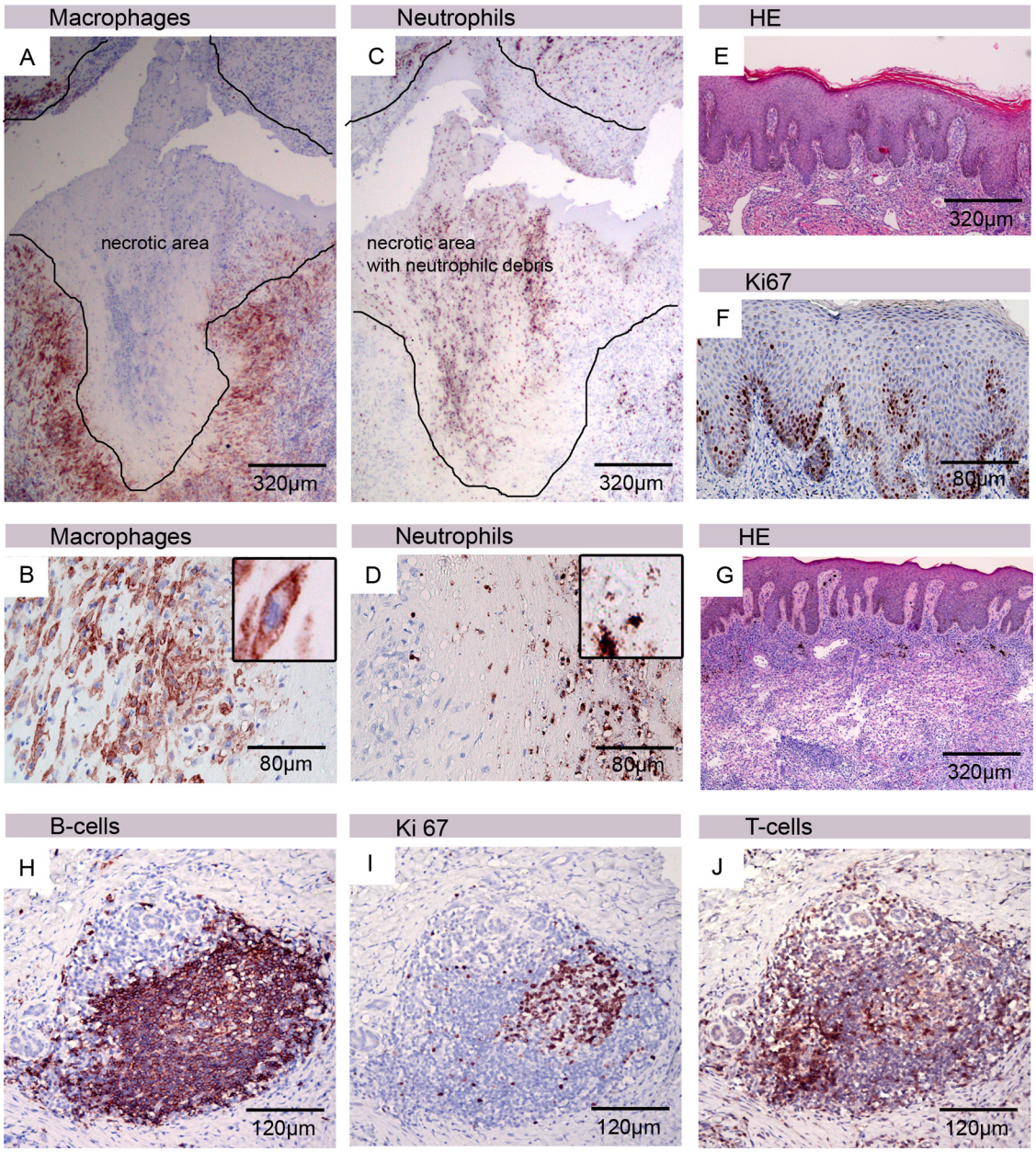

FIG 8 Features of human BU lesion with correlates in the mouse infection model. Histological sections of human tissue were stained either with hematoxylin and eosin (E and G) or with antibodies against cell surface or cytoplasmic markers and counterstained with hematoxylin (A to D, F, and H to J). A belt of intact macrophages surrounded the necrotic core (A), with neutrophilic debris from the initial wave of infiltration still being detectable (C). Appendices of macrophages reaching into the necrotic core are shown in panel B. Inside the necrotic area, no intact neutrophils could be detected (D). Epidermal hyperplasia typically observed in human BU lesions (E) associated with an elevated proliferation of the keratinocytes, indicated by staining with the Ki67 proliferation marker (F). In the neighborhood of the necrotic core of the lesion, accumulations of viable leukocytes can be observed in untreated patients (G). Clusters of $CD20^+$ B cells (H), partially highly proliferating (I) and interspersed with a few $CD3^+$ T cells (J), typically develop in the lesions of BU patients during and after completion of chemotherapy.

organized chronic infiltration type. Macrophages and neutrophils formed tight clusters around AFB, and dense lymphocyte clusters mainly consisting of $CD45R^+$ B cells developed nearby. Also in human BU lesions, structured accumulations of immune cells, including large CD20-positive B-cell clusters (Fig. 8H), develop during the course of chemotherapy (35). However, contrary to what is observed during antibiotic treatment of human BU lesions, we found no granuloma formation in the mouse footpads. Whether this lack of granuloma formation is related to the mouse strain used remains to be elucidated.

Already 1 week after start of the antibiotic treatment, incomplete ZN staining of the mycobacteria was observed, giving them a beaded appearance. In *M. tuberculosis* and *M. leprae*, beading seems to be an indicator of a loss of viability (22). In *M. leprae*, the morphological index (MI) is therefore used to determine the effectiveness of the antibiotic treatment. Ultrastructural visualiza-

tion of *M. leprae* showed that in untreated patient samples, the majority of the bacilli showed a solid staining and the cell bodies were filled homogenously with cytoplasm. In contrast, irregular ZN-stained bacilli from treated patients showed an intact cell wall but a cytoplasm which was detached from the cell wall and also showed in later stages a complete degeneration of all structures (22). Beading was also detected in samples from untreated mice at the periphery of the lesions, where bacteria were found intracellularly or in close contact with phagocytes. This and similar findings in human lesions suggest that the immune system has the capacity to kill dispersed *M. ulcerans* bacteria and that development of microcolonies surrounded by a protective cloud of mycolactone is a critical step in the establishment of a chronic *M. ulcerans* infection. After completion of treatment, AFB throughout the whole footpad revealed a beaded structure, and cultures went negative, supporting the hypothesis of beading as a marker for loss of viability. Osteomyelitis is a major severe complication occurring in >10% of all BU patients (31, 39). We observed in 15% of all mouse footpads examined bacterial infiltration in the bone marrow (data not shown), but with antibiotic treatment, these bacteria had a beaded appearance, indicating effective treatment.

Single culture-positive footpads were still found after 6 and 8 weeks of chemotherapy, and only after 10 and 12 weeks were all footpads culture negative. Although clinical trials also indicate that some bacilli may survive the recommended 8-week course of antibiotic treatment (28, 33), recurrence rates after RIF-STR treatment are as low as 1 to 2%. This indicates that immune responses primed by antigens and immunostimulators released during chemotherapy by killed bacilli are strong enough to eliminate residual dispersed bacilli (32).

ACKNOWLEDGMENTS

We thank Vincent Romanet, Caroline Fux, Melanie Stikker, Pia Wittlin, Annamaria Quadri, and Peter Schmid from Novartis, Basel, for constant help and support during sample processing and evaluation of new methods in the field of histology.

The work at the Bactériologie-Hygiène Laboratory, Faculté de Médecine Pierre et Marie Curie, Paris, France, was supported by the Fondation Raoul Follereau, France. Facilities at UPMC Université Paris 06, ER5, EA 1541, Laboratoire de Bactériologie-Hygiène, F-75005 Paris, France, are supported by a grant from Foundation Raoul Follereau, Paris, France. Histopathological analyses were supported by the Stop Buruli Initiative funded by the UBS-Optimus Foundation.

The authors have no conflicts of interest.

REFERENCES

1. **Adusumilli S, et al.** 2005. Mycobacterium ulcerans toxic macrolide, mycolactone modulates the host immune response and cellular location of M. ulcerans in vitro and in vivo. Cell. Microbiol. **7**:1295–1304.
2. **Amofah G, et al.** 2002. Buruli ulcer in Ghana: results of a national case search. Emerg. Infect. Dis. **8**:167–170.
3. **Chauty A, et al.** 2007. Promising clinical efficacy of streptomycin-rifampin combination for treatment of Buruli ulcer (Mycobacterium ulcerans disease). Antimicrob. Agents Chemother. **51**:4029–4035.
4. **Chauty A, et al.** 2011. Oral treatment for Mycobacterium ulcerans infection: results from a pilot study in Benin. Clin. Infect. Dis. **52**:94–96.
5. **Coutanceau E, et al.** 2005. Modulation of the host immune response by a transient intracellular stage of Mycobacterium ulcerans: the contribution of endogenous mycolactone toxin. Cell. Microbiol. **7**:1187–1196.
6. **Debacker M, et al.** 2004. Mycobacterium ulcerans disease (Buruli ulcer) in rural hospital, Southern Benin, 1997–2001. Emerg. Infect. Dis. **10**: 1391–1398.
7. **Dega H, et al.** 2000. Mycobacterium ulcerans infection. Ann. Med. Interne (Paris) **151**:339–344. (In French.)
8. **Diaz D, et al.** 2006. Use of the immunodominant 18-kilodalton small heat shock protein as a serological marker for exposure to Mycobacterium ulcerans. Clin. Vaccine Immunol. **13**:1314–1321.
9. **Durnez L, et al.** 2010. Terrestrial small mammals as reservoirs of Mycobacterium ulcerans in Benin. Appl. Environ. Microbiol. **76**:4574–4577.
10. **Eddyani M, et al.** 2004. Potential role for fish in transmission of Mycobacterium ulcerans disease (Buruli ulcer): an environmental study. Appl. Environ. Microbiol. **70**:5679–5681.
11. **Fyfe JAM, et al.** 2010. A major role for mammals in the ecology of Mycobacterium ulcerans. PLoS Negl. Trop. Dis. **4**:e791.
12. **Guarner J, et al.** 2003. Histopathologic features of Mycobacterium ulcerans infection. Emerg. Infect. Dis. **9**:651–656.
13. **Hayman J.** 1993. Out of Africa: observations on the histopathology of Mycobacterium ulcerans infection. J. Clin. Pathol. **46**:5–9.
14. **Hayman J, McQueen A.** 1985. The pathology of Mycobacterium ulcerans infection. Pathology **17**:594–600.
15. **Ji B, et al.** 2009. Impacts of dosing frequency of the combination rifampin-streptomycin on its bactericidal and sterilizing activities against Mycobacterium ulcerans in mice. Antimicrob. Agents Chemother. **53**: 2955–2959.
16. **Ji B, Chauffour A, Robert J, Jarlier V.** 2008. Bactericidal and sterilizing activities of several orally administered combined regimens against Mycobacterium ulcerans in mice. Antimicrob. Agents Chemother. **52**: 1912–1916.
17. **Ji B, Chauffour A, Robert J, Lefrançois S, Jarlier V.** 2007. Orally administered combined regimens for treatment of Mycobacterium ulcerans infection in mice. Antimicrob. Agents Chemother. **51**:3737–3739.
18. **Ji B, et al.** 2006. In vitro and in vivo activities of rifampin, streptomycin, amikacin, moxifloxacin, R207910, linezolid, and PA-824 against Mycobacterium ulcerans. Antimicrob. Agents Chemother. **50**:1921–1926.
19. **Johnson PDR, et al.** 2005. Buruli ulcer (M. ulcerans infection): new insights, new hope for disease control. PLoS Med. **2**:e108.
20. **Kibadi K, et al.** 2010. Response to treatment in a prospective cohort of patients with large ulcerated lesions suspected to be Buruli Ulcer (Mycobacterium ulcerans disease). PLoS Negl. Trop. Dis. **4**:e736.
21. **Kim SH, Kook MC, Shin YK, Park SH, Song HG.** 2004. Evaluation of antigen retrieval buffer systems. J. Mol. Hist. **35**:409–416.
22. **Kumar V.** 2004. High resolution shadowing of Mycobacterium leprae. Biotech. Histochem. **79**:197–201.
23. **Lefrançois S, Robert J, Chauffour A, Ji B, Jarlier V.** 2007. Curing Mycobacterium ulcerans infection in mice with a combination of rifampin-streptomycin or rifampin-amikacin. Antimicrob. Agents Chemother. **51**:645–650.
24. **Marsollier L, et al.** 2002. Aquatic insects as a vector for Mycobacterium ulcerans. Appl. Environ. Microbiol. **68**:4623–4628.
25. **Marsollier L, et al.** 2004. Aquatic snails, passive hosts of Mycobacterium ulcerans. Appl. Environ. Microbiol. **70**:6296–6298.
26. **Marsollier L, et al.** 2004. Aquatic plants stimulate the growth of and biofilm formation by Mycobacterium ulcerans in axenic culture and harbor these bacteria in the environment. Appl. Environ. Microbiol. **70**: 1097–1103.
27. **Merritt RW, et al.** 2010. Ecology and transmission of Buruli ulcer disease: a systematic review. PLoS Negl. Trop. Dis. **4**:e911.
28. **Nienhuis WA, et al.** 2010. Antimicrobial treatment for early, limited Mycobacterium ulcerans infection: a randomised controlled trial. Lancet **375**:664–672.
29. **Portaels F, et al.** 2001. Mycobacterium ulcerans in wild animals. Rev. Sci. Tech. **20**:252–264.
30. **Portaels F, Elsen P, Guimaraes-Peres A, Fonteyne PA, Meyers WM.** 1999. Insects in the transmission of Mycobacterium ulcerans infection. Lancet **353**:986.
31. **Portaels F, et al.** 2004. Mycobacterium bovis BCG vaccination as prophylaxis against Mycobacterium ulcerans osteomyelitis in Buruli ulcer disease. Infect. Immun. **72**:62–65.
32. **Ruf M-T, et al.** 2011. Secondary Buruli ulcer skin lesions emerging several months after completion of chemotherapy: paradoxical reaction or evidence for immune protection? PLoS Negl. Trop. Dis. **5**:e1252.
33. **Sarfo FS, et al.** 2010. Clinical efficacy of combination of rifampin and streptomycin for treatment of Mycobacterium ulcerans disease. Antimicrob. Agents Chemother. **54**:3678–3685.
34. **Schütte D, UmBoock A, Pluschke G.** 2009. Phagocytosis of Mycobacte-

rium ulcerans in the course of rifampicin and streptomycin chemotherapy in Buruli ulcer lesions. Br. J. Dermatol. **160**:273–283.
35. **Schütte D, et al.** 2007. Development of highly organized lymphoid structures in Buruli ulcer lesions after treatment with rifampicin and streptomycin. PLoS Negl. Trop. Dis. **1**:e2.
36. **Silva MT, Portaels F, Pedrosa J.** 2009. Pathogenetic mechanisms of the intracellular parasite Mycobacterium ulcerans leading to Buruli ulcer. Lancet Infect. Dis. **9**:699–710.
37. **Sizaire V, Nackers F, Comte E, Portaels F.** 2006. Mycobacterium ulcerans infection: control, diagnosis, and treatment. Lancet Infect. Dis. **6**:288–296.
38. **Thangaraj HS, Evans MR, Wansbrough-Jones MH.** 1999. Mycobacterium ulcerans disease; Buruli ulcer. Trans. R. Soc. Trop. Med. Hyg. **93**:337–340.
39. **Toll A, et al.** 2005. Aggressive multifocal Buruli ulcer with associated osteomyelitis in an HIV-positive patient. Clin. Exp. Dermatol. **30**:649–651.
40. **Torrado E, et al.** 2007. Evidence for an intramacrophage growth phase of Mycobacterium ulcerans. Infect. Immun. **75**:977–987.
41. **Vandelannoote K, et al.** 2010. Application of real-time PCR in Ghana, a Buruli ulcer-endemic country, confirms the presence of Mycobacterium ulcerans in the environment. FEMS Microbiol. Lett. 304:191–194.
42. **van der Werf TS, van der Graaf WT, Tappero JW, Asiedu K.** 1999. Mycobacterium ulcerans infection. Lancet **354**:1013–1018.
43. **van der Werf TS, et al.** 2005. Mycobacterium ulcerans disease. Bull. World Health Organ. **83**:785–791.
44. **WHO.** 2001. Buruli ulcer. Diagnosis of Mycobacterium ulcerans disease. WHO/CDS/CPE/GBUI/2001.4. World Health Organization, Geneva, Switzerland.
45. **World Health Organization.** 2004. Provisional guidance on the role of specific antibiotics in the managment of Mycobacterium ulcerans disease. World Health Organization, Geneva, Switzerland.